Development of Wireless Sensor Networks for Agricultural Monitoring

L. Bencini[1], S. Maddio[1], G. Collodi[1], D. Di Palma[1], G. Manes[1], and A. Manes[2]

[1] Department of Electronics and Telecommunication - University of Florence, Via di S. Marta 3, 50139 Florence, Italy
name.surname@unifi.it

[2] Netsens S.r.l., Via Tevere 70, 50019, Florence, Italy
name.surname@netsens.it

1 Introduction

The concept of precision agriculture has been around for some time now. Blackmore et al., in 1994 [1] defined it as a comprehensive system designed to optimize agricultural production by carefully tailoring soil and crop management to correspond to the unique condition found in each field while maintaining environmental quality. The early adopters during that time found precision agriculture to be unprofitable and the instances in which it was implemented were few and far between. Further, the high initial investment in the form of electronic equipment for sensing and communication meant that only large farms could afford it. The technologies proposed at this point comprised three aspects: *Remote Sensing* (RS), *Global Positioning System* (GPS) and *Geographical Information System* (GIS). RS coupled with GPS coordinates produced accurate maps and models of the agricultural fields. The sampling was typically through electronic sensors such as soil probes and remote optical scanners from satellites. The collection of such data in the form of electronic computer databases gave birth to the GIS. Statistical analyses were then conducted on the data and the variability of agricultural land was charted with respect to its properties. The technology, apart from being non-real-time, involved the use of expensive technologies like satellite sensing and was labor intensive where the maps charting the agricultural fields were mostly manually done.

Over the last seven years, the advancement in sensing and communication technologies has significantly brought down the cost of deployment and running of a feasible precision agriculture framework. Emerging wireless technologies with low power needs and low data rate capabilities have been developed which perfectly suit precision agriculture [2]. The sensing and communication can now be done on a real-time basis leading to better response times. The wireless sensors are cheap enough for wide spread deployment and offer robust communication through redundant propagation paths [3]. Thanks to these features, the *Wireless Sensor Networks* (WSNs) [3] have become the

S.C. Mukhopadhyay (Ed.): Smart Sensing Technology for Agric. & Environ. Monit., LNEE 146, pp. 157–186.
springerlink.com

most suitable technology to fit an invasive method of monitoring the agricultural environment.

The requirements that adopting a WSN are expected to satisfy in effective agricultural monitoring concern both *system level* issues (i.e., unattended operation, maximum network life time, adaptability or even self-reconfigurability of functionalities and protocols) and *final user* needs (i.e., communication reliability and robustness, user friendly, versatile and powerful graphical user interfaces). The most relevant mainly concerns the supply of *stand-alone* operations. To this end, the system must be able to run unattended for a long period, as nodes are expected to be deployed in zones that are difficult to maintain. This calls for optimal energy management. An additional requirement is *robust* operative conditions, which needs fault management since a node may fail for several reasons. Other important properties are scalability and adaptability of the network's topology, in terms of the number of nodes and their density in unexpected events with a higher degree of responsiveness and reconfigurability. Finally, several user-oriented attributes, including fairness, latency, throughput and enhanced data querying schemes need to be taken into account even if they could be considered secondary with respect to our application purposes because the WSN's cost/performance trade-off.

The before mentioned requirements call for a carefully designed and optimized overall system for the case study under consideration.

The proposed WSN system, shown in Fig. 1, is comprised of a self-organizing WSN endowed with sensing capabilities, a GPRS Gateway which gathers data and provides a TCP-IP based connection toward a Remote Server and a Web Application which manages information and makes the final user capable of monitoring and interacting with the instrumented environment.

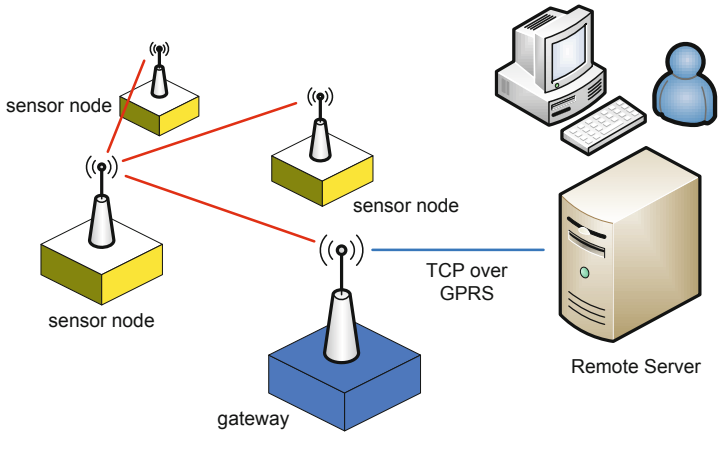

Fig. 1 Wireless Sensor Network System

In this chapter an overview of the overall system is provided. In particular Sections 2, 4 and 5 deal respectively with the system in terms of hardware, protocol and software design. Section 3 is dedicated to a detailed description of the design of directional antennas. Section 6 describes the actual experiences, focusing on several case study analyses for highlighting the effectiveness and accurateness of the developed system. Sections 7 and 8 describe respectively the commercial system "VineSense", born from the experimental solution, and some agronomic results. Finally, in Section 9 some conclusions are drawn in order to explain the future direction of the current research study.

2 Hardware Design: Sensor Nodes and GPRS Gateway

Focusing on an end-to-end system architecture, every constitutive element has to be selected according to application requirements and scenario issues, especially regarding the hardware platform. Many details have to be considered, involving the energetic consumption of the sensor readings, the power-on and power-save status management and a good trade-off between the maximum radio coverage and the transmitted power. After an accurate investigation of the out-of-the-shelf solutions, 868 MHz *Mica2 motes* [4] were adopted according to these constraints and to the reference scenarios. The *Tiny Operative System* (TinyOS) running on this platform ensures full control of mote communication capabilities to attain optimized power management and provides necessary system portability towards future hardware advancements or changes. Nevertheless, Mica2 motes are far from perfection, especially in the RF section, since the power provided by the transceiver (*Chipcon CC1000*) is not completely available for transmission. However, it is lost to imperfect coupling with the antenna, thus reducing the radio coverage area. An improvement of this section was performed, using directive antennas, described in Section 3, and coupling circuits and increasing the transmitting power with a power amplifier, thus increasing the output power up to 15 dBm while respecting international restrictions and standards. These optimizations allow for greater radio coverage (about 200 m) and better power management. In order to manage different kinds of sensors, a compliant sensor board was adopted, allowing up to 16 sensor plugs on the same node;, this makes a single mote capable of sensing many environmental parameters at a time [5]. Sensor boards recognize the sensors and send *Transducer Electronic Datasheets* (TEDS) through the network up to the server, making it possible for the system to recognize an automatic sensor. The overall node stack architecture is shown in Fig. 2.

The GPRS embedded Gateway, shown in Fig. 3, is a stand-alone communication platform designed to provide transparent, bi-directional wireless TCP-IP connectivity for remote monitoring. In conjunction with *Remote Data Acquisition* (RDA) equipment, such as WSN, it acts when connected with a Master node or when directly connected to sensors and transducers (i.e., Stand-Alone weather station, Stand-Alone monitoring camera).

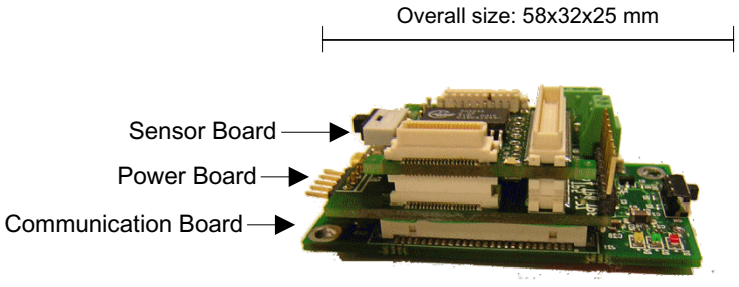

Fig. 2 Node Stack Architecture

Fig. 3 GPRS Gateway

The main hardware components that characterize the gateway are:

- a 868 MHz omnidirectional antenna;
- a miniaturized GSM/GPRS modem, with embedded TCP/IP stack [6], [7];
- a powerful 50 MHz clock microcontroller responsible for coordinating the bidirectional data exchange between the modem and the master node to handle communication with the Remote Server;
- an additional 128 KB SRAM memory added in order to allow for data buffering, even if the wide area link is lost;
- several A/D channels available for connecting additional analog sensors and a battery voltage monitor.

Since there is usually no access to a power supply infrastructure, the hardware design has also been oriented to implement low power operating modalities, using a 12 V rechargeable battery and a 20 W solar panel.

Data between the Gateway and Protocol Handler are carried out over TCP-IP communication and encapsulated in a custom protocol; from both local and remote interfaces it is also possible to access part of the Gateway's configuration settings. The low-level firmware implementation of communication

protocol also focuses on facing wide area link failures. Since the gateway is always connected with the Remote Server, preliminary connectivity experiments demonstrated a number of possible inconveniences, most of them involving the *Service Provider Access Point Name* (APN) and *Gateway GPRS Support Node* (GGSN) subsystems. In order to deal with these drawbacks, custom procedures called *Dynamic Session Re-negotiation* (DSR) and *Forced Session Re-negotiation* (FSR), were implemented both on the gateway and on the CMS server. This led to a significant improvement in terms of disconnection periods and packet loss rates.

The DSR procedure consists in a periodical bi-directional control packet exchange, aimed at verifying the status of uplink and downlink channels on both sides (gateway and CMS). This approach makes facing potential deadlocks possible if there is asymmetric socket failure, which is when one device (acting as client or server) can correctly deliver data packets on the TCP/IP connection but is unable to receive any. Once this event occurs (it has been observed during long GPRS client connections, and is probably due to Service Provider Access Point failures), the DSR procedure makes the client unit to restart the TCP socket connection with the CMS.

Instead, the FSR procedure is operated on the server side when no data or service packets are received from a gateway unit and a fixed timeout elapses: in this case, the CMS closes the TCP socket with that unit and waits for a new reconnection. On the other side, the gateway unit should catch the close event exception and start a recovery procedure, after which a new connection is re-established. If the close event should not be signaled to the gateway (for example, the FSR procedure is started during an asymmetric socket failure), the gateway would anyway enter the DSR recovery procedure.

In any case, once the link is lost, the gateway unit tries to reconnect with the CMS until a connection is re-established.

3 Directive Antennas: Design and Realization

In this section the theoretical tractation and practical implementations of directive antennas are given, while actual effects of this technology will be considered in the next sections.

3.1 Preliminaries

An antenna can be defined as a *transducer* able to converts electric energy from wired form into free-space form, and vice-versa. In a up-link, the antenna is the source of the electromagnetic field modulated by the signal provided by the transmitter, while in down-link it is the sensor which converts the impinging electromagnetic wave in a signal applied to the receiver terminals. Antenna performance is the same in either transmission and reception (*reciprocity*).

The principal figure of an antenna is the radiation pattern, which is defined as *a mathematical function or a graphical representation of the radiation properties as a function of space coordinates* [18]. Among the various radiation properties, the most important is the power density, which defines the *power pattern*, the ability of the antenna to transmit electromagnetic energy power at radio frequency. The power pattern is implicitly defined in a *far field* condition, at a distance where the radiated fields assume an almost planar wave form [21].

Complete (tridimensional) pattern of elementary antennas are typically bodies of revolution or regular surfaces. Generally one or two principal cuts would represent the entire antenna behavior. Furthermore, pattern details are emphasized with plots in dB normalized scale.

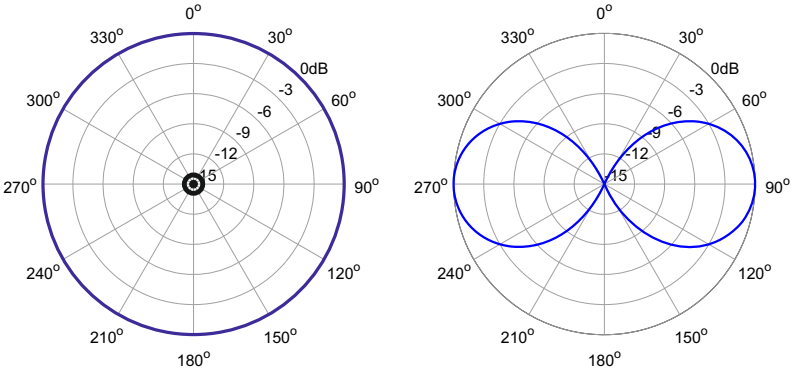

Fig. 4 Pattern of a omni-directional antenna. **Left**: top 2D cut, orthogonal to the stylus antenna; **right**: side 2D cut, containing the stylus antenna.

Real antennas of all kinds are *inherently directional*, which means that power patterns cannot be uniform. Canonical $\lambda/2$ stylus antennas are omni-directional in a 2D sense, radiating uniformly in all directions constrained in one plane, while the radiated power decreases with elevation angle above or below the antenna plane (Fig. 4). For an almost planar network, this behavior is enough to be called *omni-directional* and it is suitable for a broadcast.

In the context of this work, the term "directional" antennas refers to distinctly *directive* antennas. Following IEEE definition *the directivity is the ratio of the radiation intensity in a given direction from the antenna to the radiation intensity averaged over all directions* [20]. In particular, *maximum directivity* measures the radiation intensity of the antenna in the direction of its strongest emission.

Fig. 5 depicts a normalized pattern of a directive antenna highlighting the typical *lobes* of real devices. A radiation lobe can be defined as portion of the radiation pattern bounded by regions of relatively weak radiation intensity (radiation zeros) [18]. The principal lobe is the one containing the direction

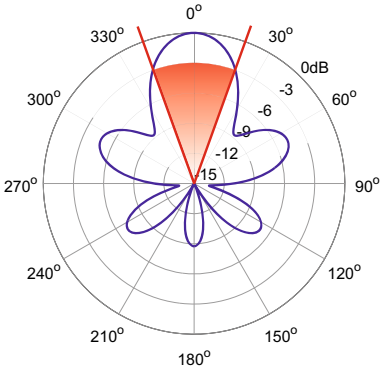

Fig. 5 Pattern of a generic antenna with a maximum in 0° and a HPBW of around 45 degree. This pattern is suitable for a fixed point-to-point transmission.

of strongest emission. An useful quantity related to the principal lobe is the Half Power Beam Width (HPBW), which is the angle between the half-power points of the lobe.

Antenna *gain* is closely related to directivity. *Gain is the ratio of the radiation intensity in a given direction, to the radiation intensity that would be obtained if the power accepted by the antenna were radiated isotropically* [20]. Gain is the product of directivity and *efficiency*, the ability to convert the available power into electromagnetic waves without waste. While directivity is a design quantity, gain is the actual quantity involved in link budget calculation.

To clarify the roles of the gain and directivity and their consequences, consider the link between two fixed antennas in far field condition. Supposing the be in a Line of Sight (LoS) condition, the link power budget is ruled by the *Friis Transmission formula* [22]:

$$P_{rx} = P_{tx} + G_{tx}(\theta, \phi) + G_{rx}(\theta, \phi) - 20 \log R - 20 \log (4\pi/\lambda) \qquad (1)$$

Where P_{rx} and P_{tx} are the received and transmitted powers, G_{tx} and G_{rx} are the gains of transmitting and receiving antenna, R is the distance between source and target and the fourth term is a constant loss depending on the link wavelength (i.e. frequency).

Given the receiver sensibility, the higher the gains, the lesser the transmitted power necessary to guarantee the same link quality. High gain implies high directivity, which in turn means that the optimal link can be established only with a *fixed* target. Therefore a single antenna cannot be suitable for both broadcast and different point-to-point links – see Fig. 6.

Another important antenna property is *polarization*, which is defined as *the curve traced by the vector representing the instantaneous electric field radiated by the antenna along the direction of propagation* [18]. Polarization varies

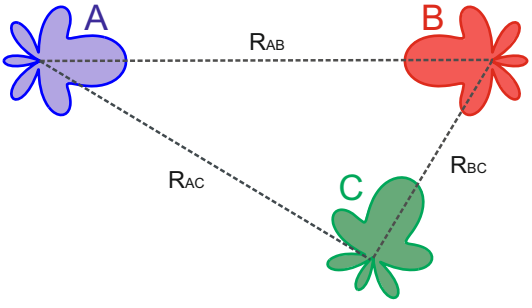

Fig. 6 Antenna links in LoS condition. AB link is optimal, with both antennas transmitting and receiving in maximum radiation. BC link is suboptimal, since only C antenna is employed in its maximum. AC link, where both antennas present a null in the link direction, represents the worst case scenario.

with direction and if not specified it is taken in the direction of maximum directivity.

It is mandatory to have the transmitting and receiving antennas matched in the polarization sense, otherwise the mismatch would reduce the signal strength acting as a negative term in Eq. 1. Circular Polarization (CP) is a particular case of polarization characterized by the electrical field describing a perfect circle. Two kind of CP's exist: Left Hand and Right Hand, which are discriminated by the rotation sense. The advantage of CP over LP is the fact that CP antennas can communicate regardless of relative orientation respect to the ground. As for linear polarization, CP antennas must be matched in the polarization sense, presenting an even higher cross-polarization rejection respect to LP case.

In a open area, the ground bouncing (two ray effect) is the principal source of *multipath*, which can severely degrade the communication quality. Cross polarization rejection candidates CP as an effective aid to contrast multipath impairments, since the radiated field by a CP antenna inverts its sense after reflecting on the ground, becoming invisible to the co-polarized receiving antenna [24].

3.2 Printed Antennas

In this work printed antennas are employed. A printed antenna, also known as patch antenna, is fabricated by photo-etching process, the same inexpensive technology of printed circuit board (PCB). As shown in Fig. 7, it consists of a very thin metallic patch printed over a layer of dielectric insulator which is in turn placed above a metallic plane serving as ground reference. For the nature of the resonant field lying between the top and the bottom metallic layers, whose configuration is named *resonant mode*, printed antennas typically exhibit the pattern maximum in the normal direction of the patch plane (broadside radiator). The best antenna performance are accomplished by properly

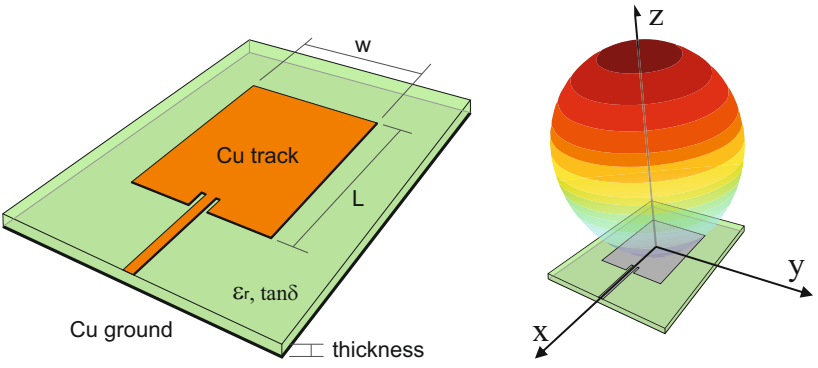

Fig. 7 Printed Antennas. **Left**: typical design for an elementary patch. **Right**: 3D Pattern shaped as a cardioid.

choosing the resonant mode of excitation beneath the patch and the opportune feeding strategy.

Printed antennas are very popular since their unique and attractive properties such as low profile, lightweight, compactness and conformability, easiness to fabricate in standard photo-etching technology and integration in MIC circuits. Not to mention the ease of analysis and syntheses with the aid of numeric C.A.D. tools. Patches typically assume the shape of squares, rectangles, circles or ellipses which are easy to analyze and fabricate, but since the 2D nature of the manufacturing procedure they can assume any arbitrary shapes, which lead to very versatile features in terms of resonant frequency, polarization, pattern shape, and input impedance.

Patches can be excited in four classical way: microstrip line, coaxial probe, aperture coupling, and proximity coupling. For the purpose of a this work, the best feeding strategies are microstrip and coaxial probe, which is particular easy to design and fabricate and demonstrates the best versatility in term of matching and polarization issue, while showing low spurious radiation.

The most basic patch is rectangular shaped as the one depicted in Fig. 7 as a $L \times W$ rectangle. The fundamental (first in the modal set) resonant mode of the patch is called TM_{01} and its centered at the frequency satisfying $L = \lambda_r/2$. It can be thought as a one-half wavelength section of open-ended microstrip transmission line (wavelength referred to the substrate). In this modal configuration the opposite sides (W-lengthed) resonate with a maximum value of the E-field, making the patch acting like a dipole. As consequence, the patch radiates a linearly polarized field, and since the presence of the ground plane, it exhibits a monolobe pattern shaped as 3D cardioid (also shown in Fig. 7) with a directivity in the range of 4-6 dB. The actual gain largely depends on substrate quality – e.g. $\tan\delta$.

Another common shape for the the patch is the disk-based. Circular geometry can achieve high compactness and better conformability than rectangular one. In the form of circular loops (Characterized by an inner and a outer radius), circular antennas present also a further degree of freedom which is useful to impose other specific characteristics to the radiator. Excited in fundamental mode – which is called TM_{11} – disc antennas are capable of almost the same radiation property of square patch, radiating a monolobe pattern and operating in linear polarization. The relationship between disk radius and resonant frequency is a little more complicated while still analytical, involving complex function like *Bessel harmonics*.

As already stated, CP antennas have proven to be successful in reducing multi-path impairments. The canonic technique to design CP patches consists in exciting two identical orthogonal modes of a symmetrical patch, but in phase quadrature. A smarter way to achieve and control the CP effect is the *modal degeneration*. With a single probe feeding a *quasi-symmetrical* shaped patch is possible to excite two overlapping modes at the same time.

The degenerated modes have to be geometrically orthogonal, and it is necessary a controllable asymmetry to detune them imposing the opportune overlap of frequency responses. Taken individually, each mode is linearly polarized – as the TM_{01} and TM_{10} of a rectangular patch – but excited at the same time, they generated two almost identical fields which can be combine in quadrature at an intermediate frequency. This fact generate a CP far-field by definition.

The modal degeneration strategy leads to compact while effective radiators, but it is successful only if the patch is asymmetric enough to support two modes resonating at two proximate center frequencies, but not too much asymmetric to separate the modes and behave too different.

Given the disk shape as basic shape, a convenient way to control the degeneration effect consists in using a central elliptical cut as a detuning element [23]. This can be considered also a deformation of a printed circular loop. While the disc radius is the main parameter for the determination of the central frequency, the ellipse axis synthesize and control the two degenerated modal frequencies. By an appropriate placement of the probe in an intermediate position between the axes of the two detuned modes, the modal fields combine in quadrature. Since a canonical disc patch antenna working in the fundamental TM_{11} mode exhibits a mono-lobe radiation pattern, the combination of the two modes will also present the same pattern behavior.

This design principle is adopted for the antennas employed in this work. The resulting antenna layout designed in common FR4 substrate ($\epsilon_r = 4.4$, $h = 1.6\,\text{mm}$, $\sigma_{Cu} = 5.8\,mS$) and its dimensions, along with the prototype photograph, are shown in Fig. 8. Dimensions and performance were traded off to be the most compact possible. The ground plane antenna element is taken only slightly larger than the patch dimension, although its limited extension leads to unavoidable coupling among other structures of the device. Anyway, the influence of actual ground dimensions and characteristics are implicitly considered in the simulation stage.

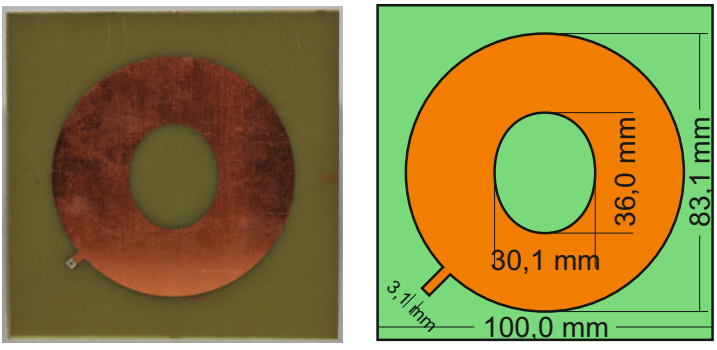

Fig. 8 Design and photograph of the proposed patch antenna.

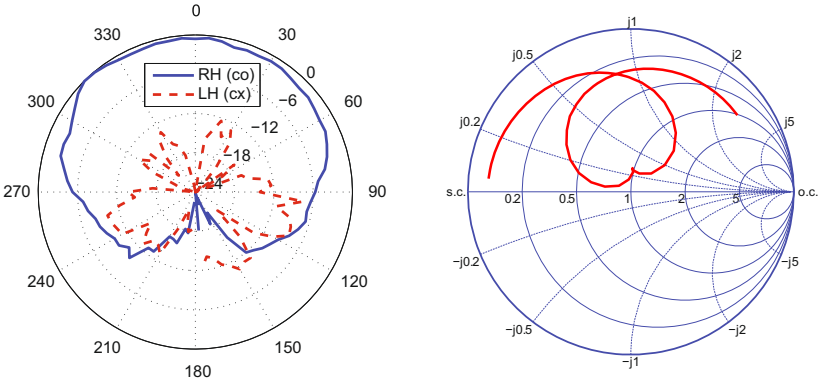

Fig. 9 Prototype characteristics. **Left**: co- and cross- polarized patterns. **Right**: smithchart with input impedance characteristics.

In Fig.9 the measured radiation pattern is demonstrated in the azimuthal plane at the design frequency of 868 MHz. The measurements reveal the good discriminations of co-poloarized and cross-polarized probe antennas (exceding 24 dB in maximum direction). Perfect CP can be achieved exactly only in the broad-side direction since axial ratio deteriorates toward horizon. The absolute gain value, estimated as 2.85 dB, is affected by the sub-optimum low-cost substrate adopted for the prototype manufacturing. In the same figure the return loss is also shown in smith chart form, revealing a minimum around the center of the plot, thus confirming the good matching. The traces exhibits a cusp at the minimum, which is a hint of the modal degeneration achieved at the design frequency.

3.3 Switched Beam Antenna

Switched beam antennas (SBA) are devices categorized as smart antenna technologies. A SBA consists of an antenna array and a beamforming network and it is capable of a predetermined set of beams which can be selected with an appropriate digital control. This technology is the complementary of *adaptive beamformer*, an array combined with a phase-shifting device, which is able to adaptively generate the required radiation pattern pointing in arbitrary direction.

Even if limited by the available set (sectorised domain), switched beam antenna are simpler – and cheaper – than adaptive beamformers, while maintaining similar advantages. The simplest beamforming network consists of a Single Pole N through (SPNT) switch. A transceiver connected to a SPNT feeding an array of N patch antennas arranged to cover the entire angular domain of interest forms the simplest SBA node. Almost all modern transceivers are equipped with a set of IO signals suitable for controlling SPNT inputs.

In figure Fig.11 is depicted a Four Beam Antenna (FBA), proposed as the basic node of the WSN. The four sector beams of the 4BA are also shown. The radiation patterns are measured in operative condition, with the antenna elements connected to the switch. The maximum gain is estimated as 2 dB, a low value affected by the switch insertion loss and unavoidable co-channel coupling. The advantages in generating 4 beams is that the cumulative pattern can cover the entire 2D angular range with a cubic box arrangement, but dedicated links can be established toward the four directions. This omnidirectional covering effect is radically different than the one given by omnidirectional antennas as the one in Fig.4.

Remembering eq. 1, the opportune beam/sector can be activated in response to the needs of the network protocol, and each of the pointing beams can be arbitrary narrow as long as the beam number is higher enough, with consequent reduction of interferences. In general, given a basic antenna element characterized by a $HPBW = \Delta\phi$, a number equal or higher than $N = 2\pi/\Delta\phi$ antennas is enough to guarantee a cumulative pattern whose HPBW is the entire 2π angle. The proposed antenna prototype adopts the family of non-reflective SPNT's by Hittite, in particular the SP4T model HMC182S14 which exhibits moderate insertion loss of 0.6 dB (over the channels) and an isolation in excess of than 40 dB for all the application of interest (see Fig.10). The adoption of this kind of non-reflective switch minimizes the interaction between elements. In fact, the matched loads connected to the idle antennas permits to dissipate the coupled signal between elements rather than reirradiate it back, thus resulting in a minimal corruption of the pattern when compared to the isolated element case.

The proposed system is capable of another smart effect. Considering the specular symmetry of the patch element, there are always two equivalent choices for the probe position respect the slitting ellipse: one for excite Left-hand circular polarization, and one for the opposite Right-Hand. A part for

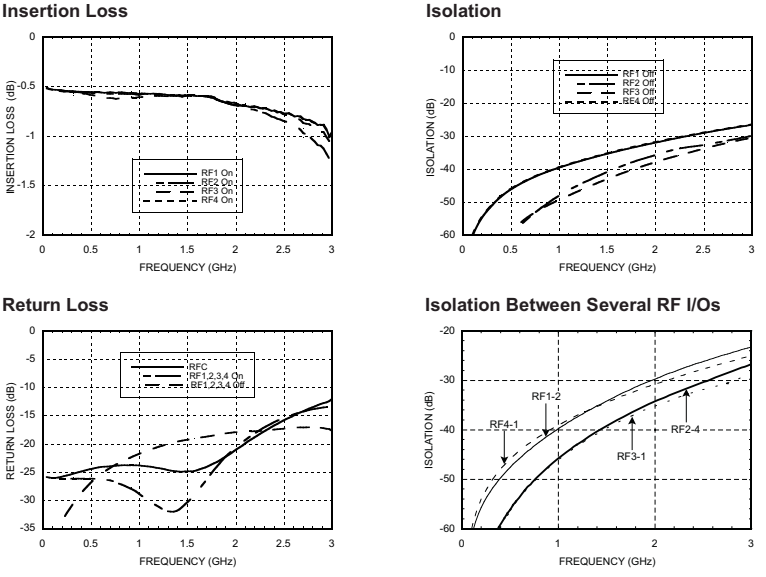

Fig. 10 HMC182S14 datasheet extract. The Single Pole 4 Through behavior versus frequency is highlighted.

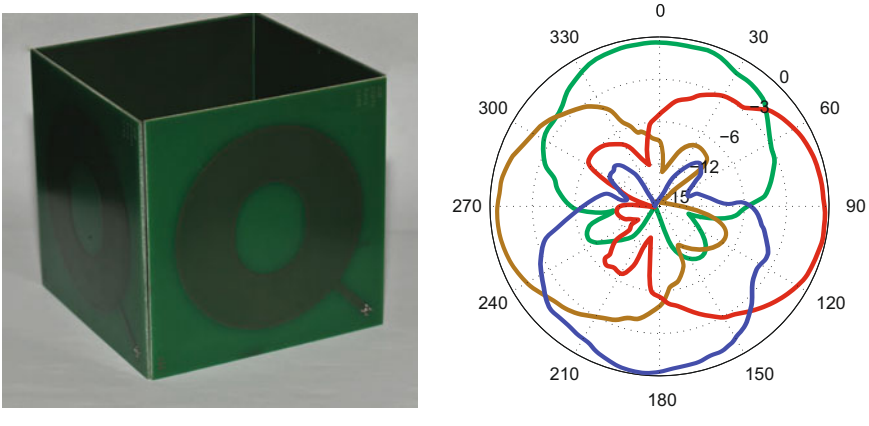

Fig. 11 Four Beam Antenna. **left**. Photograph of the a 4BA node. **Right**: Synoptic view of the four antenna beams.

the rotation sense, the radiative performance of the antenna are theoretically the same. Considering this feature, it is possible to make each antennas a reconfigurable device by the means of a second SP2T connected the two feeds points. The smart use of polarization reconfigurability can double the channel capacitance.

4 Protocol Design: A Cross-Layer Solution

The most relevant system requirements, which lead the design of an efficient Medium Access Control (MAC) and routing protocol for an environmental monitoring WSN, mainly concern power consumption issues and the possiblity of a quick set-up and end-to-end communication infrastructure that supports both synchronous and asynchronous queries. The most relevant challenge is to make a system capable of running unattended for a long period, as nodes are expected to be deployed in zones that are difficult to maintain. This calls for optimal energy management since a limited resource and node failure may compromise WSN connectivity. Therefore, the MAC and the network layer must be perfected ensuring that the energy used is directly related to the amount of handled traffic and not to the overall working time. Other important properties are scalability and adaptability of network topology, in terms of number of nodes and their density. As a matter of fact, some nodes may either be turned off may join the network afterward.

Taking these requirements into account, a *cross-layer* MAC protocol and a routing protocol were implemented.

4.1 MAC Layer Protocol

Taking the IEEE 802.11 Distributed Coordination Function (DCF) [8] as a starting point, several more energy efficient techniques have been proposed in literature to avoid excessive power waste due to so called idle listening. They are based on periodical preamble sampling performed at the receiver side in order to leave a low power state and receive the incoming messages, as in the WiseMAC protocol [9]. Deriving from the classical contention-based scheme, several protocols (S-MAC [10], TMAC [11] and DMAC [12]) have been proposed to address the overhead idle listening by synchronizing the nodes and implementing a duty cycle within each slot.

The proposed MAC protocol, called *Directive Synchronous Transmission Asynchronous Reception* (D-STAR), takes the benefits of both WiseMAC and S-MAC schemes and the features of directive antennas. It joins the power saving capability, due to the introduction of a duty-cycle, together with the advantages provided by the offset scheduling without an excessive signaling overhead. In particular, it permits to realize a *space-time* synchronization: each node periodically sends to its neighbors when it will be again in the listening status (*time synchronization*); the destination node, upon the reception of a packet, can identify the relative angular position of the sender with respect to its own angular reference system (*space synchronization*).

D-STAR protocol is characterized by the state diagram shown in Fig. 12.

According to it, each node wakes up independently, entering an initial idle state (*init state*) in which it remains for the time interval necessary for performing the elementary CPU operations and to be completely switched on

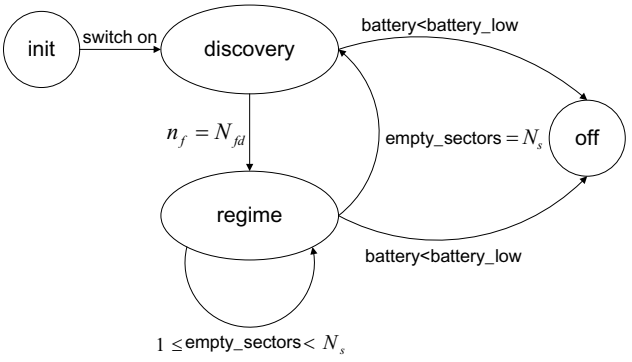

Fig. 12 Finite state machine description of the proposed D-STAR protocol for mesh networks, involving the transitions occurring among *init*, *discovery*, *regime* and *off* states.

(T_{init}). Moreover, before entering the *discovery state*, each node starts to organize the time into frames whose durations are T_f.

In the *discovery state* each node tries to identify its neighbors and to establish a *time-space* synchronization with them. To this purpose it remains in a listening mode for a time interval equal to $T_{set-up} \geq 2T_f$ and begins to periodically broadcast a HELLO message to each angular sector (i.e., the coverage area within a certain side lobe) sending its *ID* and its *phase*. The phase is the time interval after which the sender exits from the *discovery state*, enters the *regime state* and changes back in listening mode in that particular sector. A node that receives a HELLO message adds the source node to the list of its own active neighbors and transmits an acknowledgement.

The overall messages exchanged during the *discovery state* are represented in Fig. 13. It is assumed that Node A has two neighbors belonging to two different angular sectors. Node A begins the channel sensing procedure and then it sends one HELLO message per angular sector. Upon the successful reception of this message, each node adds Node A to the list of its own active neighbors. The procedure is repeated until the *discovery state* is expired. This condition can be alternatively expressed as $n_f = N_{fd}$, where n_f is the number of frame periods spent from the beginning of the *discovery state* and N_{fd} represents its maximum value.

Once the *discovery state* has expired, each node enters the *regime state*. Within this state the operation mode is duty cycled with a periodic alternation of listening and sleeping sub-periods whose time intervals are T_l and T_s respectively. The duty cycle function is given by the following formula:

$$d = \frac{T_l}{T_l + T_s} \tag{2}$$

In the *regime state* each node tries to preserve the synchronization with its neighbors. To this purpose it sends a frame-by-frame HELLO message in

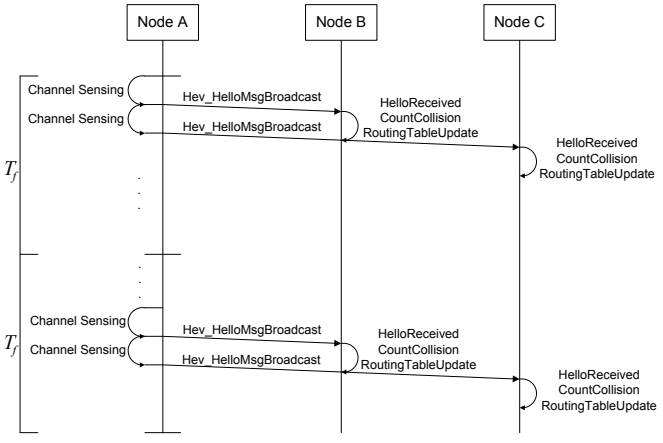

Fig. 13 Messages exchange during the *discovery state*

a unicast way to the active nodes in its list belonged to different sectors according to the phase transmitted by them in previous HELLO messages. As in the *discovery state*, the HELLO message contains the *ID* and the *phase* that, in this case, is the time interval after which the sender claims to be again in the listening status in that sector waiting for the HELLO messages. The phase ϕ is evaluated according to the following rule:

$$\phi_1 = \tau - T_l \tag{3}$$

if the node is in the sleeping mode, where τ is the time remaining to the beginning of the next frame. Conversely, if the node is in the listening status, ϕ is computed as:

$$\phi_2 = \tau + T_s \tag{4}$$

The channel access is managed using the Carrier Sense Multiple Access with the Collision Avoidance (CSMA/CA) scheme. This mechanism is very effective in reducing collisions, while the problem of hidden nodes is still partially unsolved.

Each node remains in the *regime state* until there is at least one neighbor, otherwise if there are no active neighbors (i.e., the number of empty angular sectors is equal to the number of sector N_s), it reenters the *discovery state* in search of connectivity.

To complete the protocol characterization, whenever a node battery is depleted, this node turns off entering the *off state*.

To give an insight on the protocol energy efficiency, in Fig. 14, the relative lifetime as a function of the number of network nodes is presented in the case of directive antennas with two and four angular sector, respectively, normalized to the lifetime achieved by using omnidirectional antennas. The remarkable

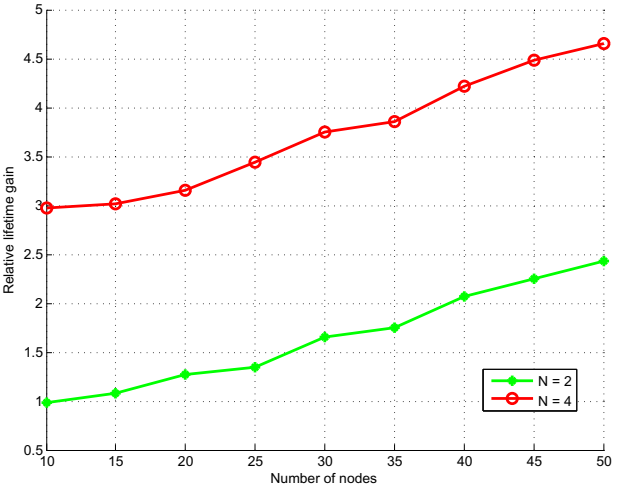

Fig. 14 Normalized network lifetime vs. Number of nodes

gain provided by the introduction of directive antennas could be noticed: in particular, it increases at the increasing of the node density (underlying an optimal scalability).

The energy efficiency of the proposed protocol can be also evaluated by focusing on the collision probability that depends upon the node density and the presence of the hidden nodes. The underlying CSMA/CA mechanism might fail indeed if neighbor nodes get extremely close or if two or more nodes not belonging to the same coverage area attempt to transmit toward the same node. To get an insight on this aspect, in Fig. 15, the collision probability as a function of the number of network nodes is depicted in the case of omnidirectional antennas and directive antennas with two and four angular sectors, respectively.

It could be noticed that the adoption of omnidirectional antennas minimizes the packets collisions as the hidden node effect is minimized. However, as the angular resolution increases, the collision probability decreases since a lower number of nodes might overlap with a third node when transmitting and the communication becomes really *point-to-point*.

To conclude this analysis, the latency is evaluated (see Fig. 16). According to this results, the omnidirectional scheme takes the longer time to deliver a packet, due to the higher probability of finding the channel busy.

4.2 Network Layer Protocol

In order to evaluate the capability of the proposed MAC scheme in establishing effective end-to-end communications within a WSN, a routing protocol was introduced and integrated according to the *cross layer* design principle [13]. In

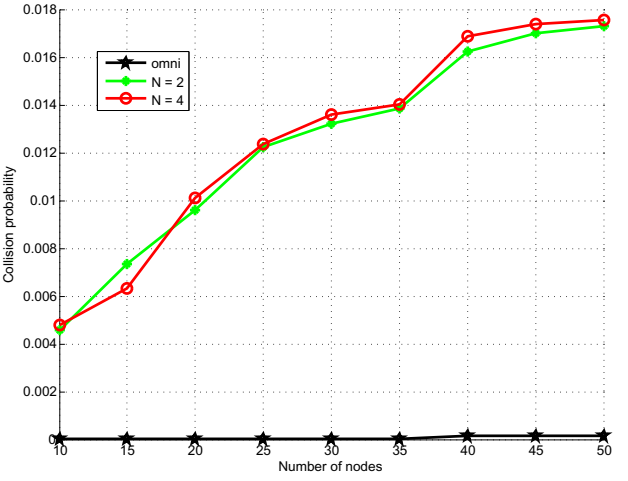

Fig. 15 Normalized network lifetime vs. Number of nodes

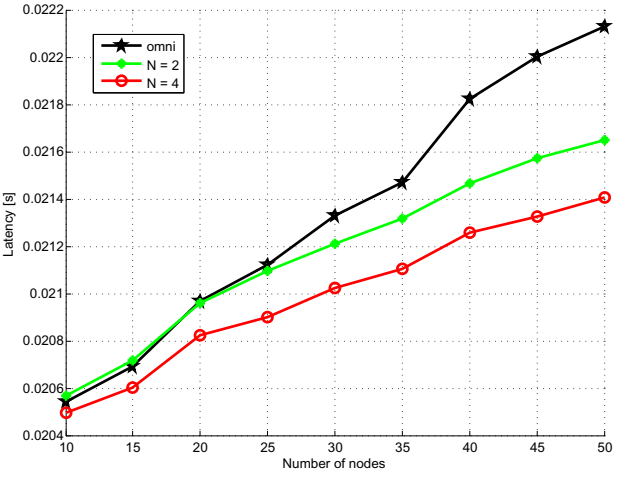

Fig. 16 Latency vs. Number of nodes

particular, we refer to a proactive algorithm belonging to the class link-state protocol that enhance the capabilities of the *Link Estimation Parent Selection* (LEPS) protocol. It is based on periodically information needed for building and maintaining the local routing table, depicted in Table 1. However, our approach resorts both to the signaling introduced by the MAC layer (i.e., synchronization message) and by the Network layer (i.e., ping message), with the aim of minimizing the overhead and make the system more adaptive in

a cross layer fashion. In particular, the parameters transmitted along a MAC synchronization message, with period T_f, are the following:

- *next hop* (NH) to reach the gateway, that is, the MAC address of the one hop neighbor;
- *distance* (HC) to the gateway in terms of number of needed hops;
- *phase* (PH) that is the schedule time at which the neighbor enter in listening mode according to Equation (3) and Equation (4);
- *sector* (SE) of the switched beam antenna that the node has to select for reaching the next hop;
- *link quality* (LQ) estimation as the ratio of correctly received and the expected synchronization messages from a certain neighbor.

Table 1 Routing Table General Structure

Target	**NH**	**HC**	**PH**	**SE**	**LQ**	**BL**	**CL**
Sink 1	A	N_A	ϕ_A	λ_A	η_A	B_A	C_A
	B	N_B	ϕ_B	λ_A	η_B	B_B	C_B
Sink 2	C	N_C	ϕ_C	λ_C	η_C	B_C	C_C
	D	N_D	ϕ_D	λ_D	η_D	B_D	C_D

On the other hand, the parameters related to long-term phenomena are carried out by the ping messages, with period $T_p \gg T_f$, in order to avoid unnecessary control traffics and, thus, reducing congestion. Particularly, they are:

- *battery level* (BL) (i.e., an estimation of the energy available at that node);
- *congestion level* (CL) in terms of the ratio between the number of packets present in the local buffer and the maximum number of packets to be stored in.

Once, the routing table has been filled with these parameters, it is possible to derive the proper metric by means of a weighted summation of them. It is worth mentioning that the routing table might indicate more than one destination (*sink*) thanks to the ping messages that keep trace of the intermediate nodes within the message header.

5 Software and End User Interface Design

The software implementation was developed, considering a node as both a single element in charge of accomplishing prearranged tasks and as a part of a complex network in which each component plays a crucial role in the network's maintenance. As far as the former aspect is concerned, several TinyOS modules were implemented for managing high and low power states and for

realizing a finite state machine, querying sensors at fixed intervals and achieving anti-blocking procedures, in order to avoid software failure or deadlocks and provide a robust stand alone system. On the other hand, the node has to interact with neighbors and provide adequate connectivity to carry the messages through the network, regardless of the destination. Consequently, additional modules were developed according to a cross layer approach that are in charge of managing D-STAR MAC and multihop protocols. Furthermore, other modules are responsible for handling and forwarding messages, coming from other nodes or from the gateway itself. Messages are not only sensing (i.e., measures, battery level) but also control and management messages (i.e., synchronization, node reset). As a result, a full interaction between the final user and the WSN is guaranteed.

The final user may check the system status through graphical user interface (GUI) accessible via web. After the log-in phase, the user can select the proper pilot site. For each site the deployed WSN together with the gateway is schematically represented through an interactive map. In addition to this, the related sensors display individual or aggregate time diagrams for each node with an adjustable time interval (Start/Stop) for the observation. System monitoring could be performed both at a high level with a user friendly GUI and at a low level by means of message logging.

Fig. 17 shows some friendly Flash Player applications that, based on mathematical models, analyze the entire amount of data in a selectable period and provide ready-to-use information. Fig. 17(a) specifically shows the aggregate data models for three macro-parameters, such as vineyard water management, plant physiological activity and pest management. The application, using cross light colors for each parameter, points out normal (green), mild (yellow) or heavy (red) stress conditions and provides suggestions to the farmer on how to apply pesticides or water in a certain part of the vineyard. Fig. 17(b) shows a graphical representation of the soil moisture measurement. Soil moisture sensors positioned at different depths in the vineyard make it possible to verify whether a summer rain runs off on the soil surface or seeps into the earth and provokes beneficial effects on the plants: this can be appreciated with a rapid look at the soil moisture aggregate report which, shows the moisture sensors at two depths with the moisture differences colore in green tones. Fig. 17(c) highlights stress conditions on plants, due to dry soil and/or to hot weather thanks to the accurate trunk diametric growth sensor that can follow each minimal variation in the trunk giving important information on plant living activity. Finally, Fig. 17(d) shows a vineyard map: the green spots are wireless units, distributed in a vineyard of one hectare.

6 Real World Experiences

The WSN system described above was developed and deployed in three pilot sites and in a greenhouse. Since 2005, an amount of 198 sensors and 50 nodes

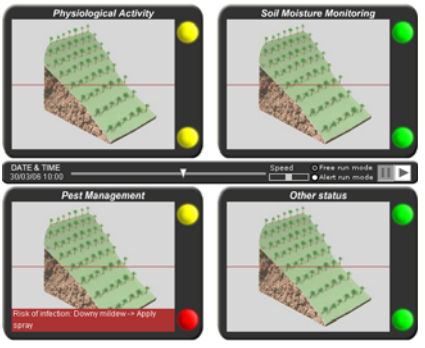

(a) Aggregate Data Models for Vineyard Water Management, Plant Physiological Activity and Pest Management

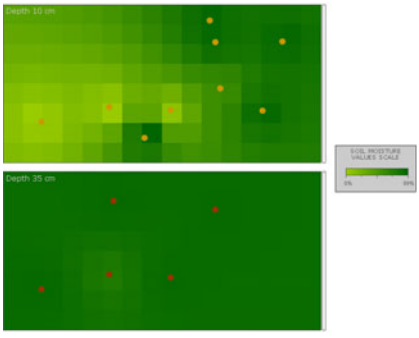

(b) Soil Moisture Aggregation Report: the upper map represent soil moisture @ 10 cm in the soil and the lower map represents soil moisture @ 35cm in the vineyard after a slipping rain

(c) Trunk Diametric Growth Diagram: daily and nightly metabolic phases

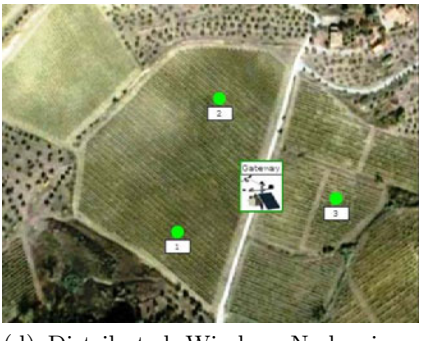

(d) Distributed Wireless Nodes in a Vineyard

Fig. 17 Flash Player User Interface

have continuously sent data to a remote server. The collected data represents a unique database of information on grape growth useful for investigating the differences between cultivation procedures, environments and treatments.

6.1 Pilot Sites Description

The first pilot site was deployed in November 2005 on a sloped vineyard of the Montepaldi farm in Chianti Area (Tuscany - Italy). The vineyard is a wide area where 13 nodes (including the master node) with 24 sensors, running D-STAR MAC and dynamic routing protocols were successfully deployed. The deployment took place in two different steps: during the first one, 6 nodes (nodes 9,10,14,15,16,17) were placed to perform an exhaustive one

Table 2 Message Delivery Rate for the Montepaldi Farm Pilot Site

Location	MDR
Node 9	72.2%
Node 10	73.7%
Node 11	88.5%
Node 12	71.4%
Node 13	60.4%
Node 14	57.2%
Node 15	45.6%
Node 16	45.4%
Node 17	92.1%
Node 18	87.5%
Node 19	84.1%

week test. The most important result regards the multi-hop routing efficiency, estimated as:

$$\eta_{MHop} = \frac{M_{EU}}{M_{ex}} \tag{5}$$

where η_{MHop} is the efficiency, M_{EU} are the messages correctly received by the remote user and M_{ex} are the expected transmitted messages. For the gateway neighbors, η_{MHop} is very high, over 90%. However, even nodes far from the gateway (i.e., concerning an end-to-end multihop path) show a message delivery rate (MDR) of over 80%. This means that the implemented routing protocol does not affect communication reliability. After the second deployment, in which nodes 11,12,13,18,19,20 were arranged, the increased number of collisions changed the global efficiency, thus decreasing the messages that arrived to the end user, except for nodes 18,19,20, in which an upgraded firmware release was implemented. The related results are detailed in Table 2.

This confirms the robustness of the network installed and the reliability of the adopted communications solution, also considering the power consumption issues: batteries were replaced on March 11^{th} 2006 in order to face the entire farming season. After that, eleven months passed before the first battery replacement occurred on February 11^{th} 2007, confirming our expectations and fully matching the user requirements. The overall Montepaldi system has been running unattended for one year and a half and is going to be a permanent pilot site. So far, nearly 2 million samples from the Montepaldi vineyard have been collected and stored in the server at the University of Florence Information Services Centre (CSIAF), helping agronomist experts improve wine quality through deeper insight on physical phenomena (such as weather and soil) and the relationship with grape growth.

The second pilot site was deployed on a farm in the Chianti Classico with 10 nodes and 50 sensors at about 500 m above sea level on a stony hill area of 2.5 hectares. The environmental variations of the the "terroir" have been

monitored since July 2007, producing one of the most appreciated wines in the world.

Finally, the third WSN was installed in Southern France in the vineyard of Peach Rouge at Gruissan. High sensor density was established to guarantee measurement redundancy and to provide a deeper knowledge of the phenomena variation in an experimental vineyard where micro-zonation has been applied and where water management experiments have been performed for studying plant reactions and grape quality.

6.2 Greenhouse

An additional deployment at the University of Florence Greenhouse was performed to let the agronomist experts conduct experiments even in seasons like Fall and Winter, where plants are quiescent, thus breaking free from the natural growth trend. This habitat also creates the opportunity to run several experiments on the test plants, in order to evaluate their responses under different stimuli using in situ sensors.

The greenhouse environmental features are completely different from those of the vineyard: as a matter of fact, the multipath propagation effects become relevant, due to the indoor scenario and the presence of a metal infrastructure. A highly dense node deployment, in terms of both nodes and sensors, might imply an increased network traffic load. Nevertheless, the same node firmware and hardware used in the vineyard are herein adopted; this leads to a resulting star topology as far as end-to-end communications are concerned.

Furthermore, 6 nodes have been in the greenhouse since June 2005, and 30 sensors have constantly monitored air temperature and humidity, plants soil moisture and temperature, differential leaf temperature and trunk diametric growth. The sensing period is equal to 10 minutes, less than the climate/plant parameter variations, providing redundant data storage. The WSN message delivery rate is extremely high: the efficiency is over 95%, showing that a low number of messages are lost.

7 VineSense: A WSN Commercial System

The fruitful experience of the three pilot sites was gathered by a new Italian company, Netsens, founded as a spinoff of the University of Florence. Netsens has designed a new monitoring system called VineSense based on WSN technology and oriented towards market and user applications.

VineSense exalts the positive characteristics of the experimental system and overcomes the problems encountered in past experiences, thus achieving an important position in the wireless monitoring market.

The first important outcome of the experimental system, enhanced by VineSense is the idea of an end-to-end system. Sensors deployed in the field constantly monitor and send measurements to a remote server through the WSN.

Data can be queried and analyzed by final users thanks to the professional and user-friendly VineSense web interface. Qualified mathematic models are applied to monitoring parameters and provide predictions on diseases and plant growth, increasing agronomists' knowledge and reducing costs while paving the road for new vineyard management.

VineSense improves many aspects of the experimental system, both in electronics and telecommunications.

The MAC and Routing protocol tested in the previous experimental system showed such important and significant results in terms of reliability that the same scheme was also adopted in the VineSense system and minimal changes were introduced: the routing protocol is lighter in terms of data exchange, building the route with different parameters, aimed at increasing the message success rate, such as master node distance and received signal strength.

A more secure data encryption was adopted in data messages to protect customers from malicious sniffing or to discourage possible competitors from decrypting network data.

Furthermore, a unique key-lock sequence was also implemented on each wireless node to prevent stealing, ensuring correct use with only genuine Netsens products and only in combination with its master node, which comes from the factory.

The new wireless nodes are smaller, more economical, more robust and suited for vineyard operations with machines and tractors. The electronics are more fault-tolerant, easier to install and more energy efficient: only a 2200 mAh lithium battery for 2-3 years of continuous running without human intervention. Radio coverage has been improved up to 350 m and nodes deployment can be easily performed by end users who can rely on a smart installation system with instantaneous radio coverage recognition. Some users have also experimented with larger area coverage, measuring a point-to-point communication of about 600 m in the line of sight.

Hypothetically, a VineSense system could be composed of up to 255 wireless nodes and more than 2500 sensors, considering a full sensor set per node, but since it is a commercial system these numbers are much more than necessary to cover farmers' needs.

Sensors used in the VineSense system are low-cost, state-of-the-art devices designed by Netsens for guaranteeing the best accuracy-reliability-price ratio. The choice of Netsens to develop custom and reliable sensors for the VineSense system is not only strategic from a marketing point of view, since it frees VineSense from any kind of external problems, such as external supplying, delays, greater costs and compliancy. It is also a consequence of the "System Vision", where VineSense is not only a wireless communication system product, but an entire system with no "black holes" inside so as to provide the customer with a complete system with better support.

Recovery strategies and communication capabilities of the stand-alone GPRS gateway have been improved: in fact, data received by wireless nodes are both forwarded in real-time to a remote server and temporarily stored

on board in case of abrupt disconnections; moreover, automatic reset and restart procedures avoid possible software deadlocks or GPRS network failures. Finally, a high-gain antenna guarantees good GPRS coverage almost everywhere.

The GPRS gateway firmware has been implemented for remotely managing of the acquisition settings, relieving users of the necessity of field maintenance.

The GPRS gateway communication has been greatly improved introducing new different communication interfaces, such as Ethernet connection (RJ-45), USB data downloading and the possibility of driving an external Wi-Fi communication system for short-range transmissions.

Since the beginning of 2010, the "Always On" connection started to be fully used and it boosted the VineSense system, enlarging its possible field of application: a complete bidirectional communication was established between the GPRS unit in the field and the remote server at Netsens. The previous "one way" data flow, from the vineyard to the internet, was gone over by a new software release, able to send instantaneous messages from the VineSense web interface to the field: the monitoring system was changed into the monitoring and control system, sending automatic, scheduled or asynchronous commands to the gateway station or to nodes, i.e. to open or close irrigation systems or simply to download a firmware upgrade.

In Fig. 18 the GPRS gateway with weather sensors is shown.

Fig. 18 VineSense GPRS Gateway with Weather Sensors

The web interface is the last part of VineSense's end-to-end: the great amount of data gathered by the sensors and stored in the database needs a smart analysis tool to become useful and usable. For this reason different tools

are at the disposal of various kinds of users. On one hand, some innovative tools such as control panels for real time monitoring or 2D chromatic maps create a quick and easy approach to the interface. On the other hand, professional plots and data filtering options allow experts or agronomists to study them more closely.

8 Agronomic Results

The use of VineSense in different scenarios with different agronomic aims has brought a large amount of important results.

When VineSense is adopted to monitor soil moisture positive effects can be obtained for plants and saving water, thus optimizing irrigation schedules. Some examples of this application can be found in systems installed in the Egyptian desert where agriculture is successful only through wise irrigation management. In such a terroir, plants suffer continuous hydric stress during daylight due to high air temperature, low air humidity and hot sandy soils with a low water retention capacity. Water is essential for plant survival and growth, an irrigation delay can be fatal for the seasonal harvest therefore, a reliable monitoring system is necessary. The adoption of VineSense in this scenario immediately resulted in continuous monitoring of the irrigating system, providing an early warning whenever pump failure occurred. On the other hand, the possibility to measure soil moisture at different depths allows agronomists to decide on the right amount of water to provide plants; depending on different day temperatures and soil moisture, pipe schedules can be changed in order to reduce water waste and increase water available for plants.

An example of different pipe schedules is shown in Fig. 19.

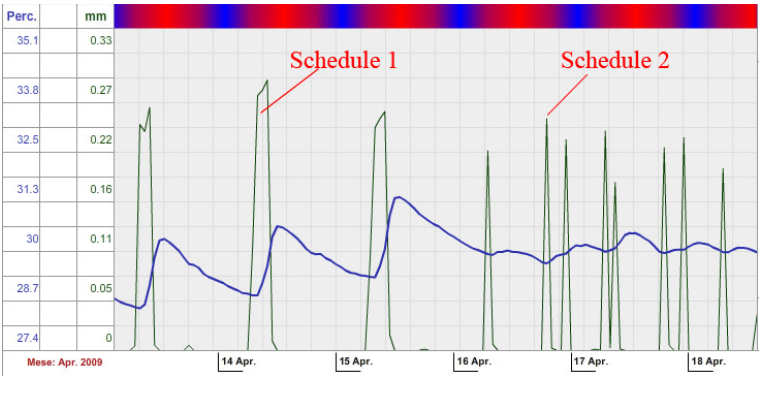

Fig. 19 Different Pipe Schedules in Accordance with Soil Moisture Levels

Originally, the irrigation system was opened once a day for 5 hours giving 20 liters per day (schedule 1); since sandy soils reach saturation very rapidly most of this water was wasted in deeper soil layers; afterwards irrigation schedules were changed (schedule 2), giving the same amount of water in two or more times per day; the water remained in upper soil layers at plant root level, reducing wastes and increasing the amount of available water for plants, as highlighted by soil moisture at 60 *cm* (blue plot).

Another important application of the VineSense system uses the dendrometer to monitor plant physiology. The trunk diametric sensor is a mechanical sensor with $+/-$ 5 microns of accuracy; such an accurate sensor can appreciate stem micro variations occurring during day and night, due to the xilematic flux inside the plant. Wireless nodes measure plant diameter every 15 minutes, an appropriate time interval for following these changes and for creating a plot showing this trend. In normal weather conditions, common physiologic activity can be recognized by agronomists the same as a doctor can do reading an electrocardiogram; when air temperature increases and air humidity falls in combining low soil moisture levels, plants change their activity in order to face water stress, preserve their grapes and especially themselves. This changed behavior can be registered by the dendrometer and plotted in the VineSense interface, warning agronomists about incoming risks; as a consequence, new irrigation schedules can be carried into effect.

Fig. 20 shows an example of a plant diametric trend versus air temperature.

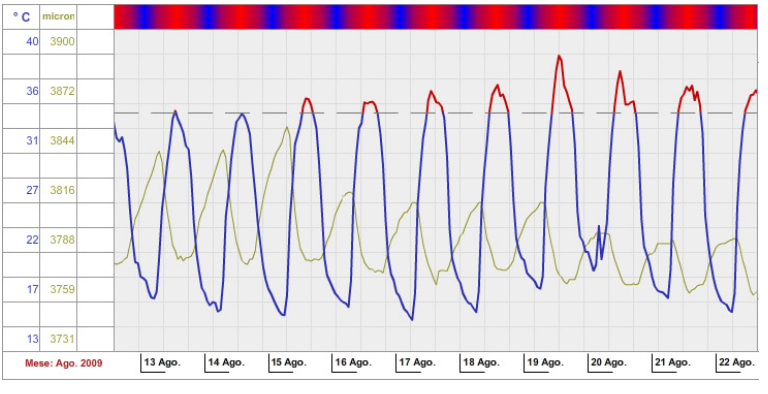

Fig. 20 Plant Diametric Trend vs. Air Temperature

The blue plot represents the air temperature in 10 days, from 13^{th} August until the 22^{nd} August 2009 in Italy; the blue line becomes red when the temperature goes over a 35 degree threshold. During the period in which the temperature is so high, plant stem variations are reduced due to the lower amount of xilematic flux flowing in its vessels, a symptom of water leakage.

WSN in agriculture are also useful for creating new databases with historical data: storing information highlighting peculiarities and differences of vineyards provides agronomists an important archive for better understanding variations in plant production capabilities and grape ripening. Deploying wireless nodes on plants in interesting areas increases the knowledge about a specific vineyard or a specific terroir, thus recording and proving the specificity of a certain wine. I.E., the quality of important wines such CRU, coming from only one specific vineyard, can be easily related to "grape history": data on air temperature and humidity, plant stress, irrigation and rain occurring during the farming season can assess a quality growing process, that can be declared to buyers.

Finally, VineSense can be used to reduce environmental impact thanks to a more optimized management of pesticides in order to reach a sustainable viticulture. Since many of the most virulent vine diseases can grow in wet leaf conditions, it is very important to monitor leaf wetness in a continuous and distributed way. Sensors deployed in different parts of vineyards are a key element for agronomists in monitoring risky conditions: since wetness can change very rapidly during the night in a vineyard and it is not homogeneous in a field, a real time distributed system is the right solution for identifying risky conditions and deciding when and where to apply chemical treatments. As a result, chemicals can be used only when they are strictly necessary and only in small parts of the vineyard where they are really needed, thus reducing the number of treatments per year and decreasing the amount of active substances sprayed in the field and in the environment. In some tests performed in 2009 in Chianti, the amount of pesticides was reduced by 65% compared to the 2008 season.

Leaf wetness sensors on nodes 2 and 3 measure different wetness conditions as shown in Fig. 21. The upper part of the vineyard is usually wetter (brown plot) than the lower part (blue plot) and sometimes leaf wetness persists for many hours, increasing the risk of attacks on plants.

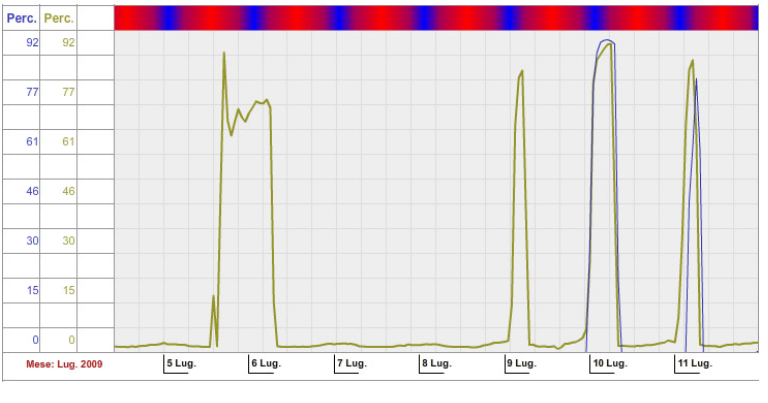

Fig. 21 Different Leaf Wetness Conditions in a Small Vineyard

9 Conclusion

This paper deals with the design, optimization and development of a practical solution for application to the agro-food chain monitoring and control. The overall system was addressed in terms of the experienced platform, network issues related both to communication protocols between nodes and gateway operations up to the suitable remote user interface. Every constitutive element of the system chain was described in detail in order to point out the features and the remarkable advantages in terms of complexity reduction and usability.

To highlight the effectiveness and accurateness of the developed system, several case studies were presented. Moreover, the encouraging and unprecedented results achieved by this approach and supported by several pilot sites into different vineyard in Italy and France were shown.

The fruitful experience of some pilot sites was gathered by a new Italian company, Netsens, founded as a spin off of the University of Florence. Netsens has designed a new monitoring system called VineSense based on WSN technology and oriented towards market and user applications. In order to point out the improvements of the new solution respect to the experimental one, the main features of VineSense were described. Moreover, some important agronomic results achieved by the use of VineSense in different scenarios were sketched out, thus emphasizing the positive effects of the WSN technology in the agricultural environment.

Nowadays, the research group is investing substantial resources on the realization of custom sensors for leaf wetness, soil moisture and soil temperature monitoring.

References

1. Blackmore, S.: Precision Farming: An Introduction. Outlook on Agriculture Journal 23, 275–280 (1994)
2. Wang, N., Zhang, N., Wang, M.: Wireless sensors in agriculture and food industry - Recent development and future perspective. Computers and Electronics in Agriculture Journal 50, 114–120 (2006)
3. Akyildiz, I.F., Xudong, W.: A Survey on Wireless Mesh Networks. IEEE Communication Magazine 43, S23–S30 (2005)
4. Mica2 Series, `http://www.xbow.com`
5. Mattoli, V., Mondini, A., Razeeb, K.M., Oynn, B., Murphy, F., Bellis, S., Collodi, G., Manes, A., Pennacchia, P., Mazzolai, B., Dario, P.: Development Agricultural Applications. In: Proc. of IE 2005. IEEE Computer and Communications Societies, Sydney (2005)
6. Sveda, M., Benes, P., Vrba, R., Zezulka, F.: Introduction to IndustrialSensor Networking. Handbook of Sensor Networks: Compact Wireless and Wired Sensing Systems, 10–24 (2005)
7. Jain, J.N., Agrawala, A.K.: Open Systems Interconnection: Its Architecture and Protocols. Elsevier (1990)

8. IEEE Standard 802.11, Wireless LAN Medium Access Control (MAC)and Physical Layer (PHY) Specifications. IEEE Computer Society (1999)
9. El-Hoiydi, A., Decotignie, J., Enz, C., Le Roux, E.: WiseMAC, an Ultra Low Power MAC Protocol for the WiseNET Wireless Sensor Network. In: Proc. of SENSYS 2003, pp. 244–251. Association for Computer Machinery, Los Angeles (2003)
10. Ye, W., Heidemann, J., Estrin, D.: An Energy-Ecient MAC Protocol for Wireless Sensor Networks. In: Proc. of INFOCOM 2002, pp. 1567–1576. IEEE Computer and Communications Societies, New York (2002)
11. Dam, T., Langendoen, K.: An Adaptive Energy-Ecient MAC Protocol for Wireless Sensor Networks. In: Proc. of SENSYS 2003, pp. 171–180. Association for Computer Machinery, Los Angeles, CA (2003)
12. Lu, G., Krishnamachari, B., Raghavendra, C.: Adaptive Energy-Ecient and Low-Latency MAC for Data Gathering in Sensor Networks. In: Proc. of WMAN 2004, pp. 2440–2443. Institut fur Medien.Informatik, Ulm, Germany (2004)
13. Shakkottai, S., Rappaport, T., Karlsson, P.: Cross-Layer Design for Wireless Networks. Proc. of IEEE Communication Magazine 41, 77–80 (2003)
14. Kipphan, H.: Handbook of printmedia. Springer, Heidelberg (2000)
15. Brandt, J., Hein, W.: Polymer materials in joint surgery. In: Grellmann, W., Seidler, S. (eds.) Deformation and Fracture Behavior of Polymers. Engineering Materials. Springer, Heidelberg (2001)
16. Che, M., Grellmann, W., Seidler, S.: Appl. Polym. Sci. 64, 1079–1090 (1997)
17. Ross, D.W.: Lysosomes and storage diseases. MA Thesis. Columbia University, New York (1977)
18. Balanis, C.A.: Antenna theory Analysis and Design, 3rd edn. Wiley, New York (1977)
19. Manabe, T., Miura, Y., Ihara, T.: Eects of antenna directivity and polarization on indoor multipath propagation characteristics at 60 GHz. IEEE Journal on Selected Areas in Communications 14(3), 441–448 (1996)
20. IEEE standard denitions of terms for antennas. IEEE Transactions on Antennas and Propagation 17(3), 262–269
21. Notaros, B.M.: Electromagnetics, pp. 720–722. Pearson (2010)
22. Notaros, B.M.: Electromagnetics, pp. 768–771. Pearson (2010)
23. Maddio, S., Cidronali, A., Manes, G.: A New Design Method for Single-Feed Circular Polarization Microstrip Antenna with an Arbitrary Impedance Matching Condition. IEEE Transactions on Antennas and Propagation 59(2), 379–389 (2011)
24. Cidronali, A., Maddio, S., Giorgetti, G., Manes, G.: Analysis and Performance of a Smart Antenna for 2.45-GHz Single-Anchor Indoor Positioning. IEEE Transactions on Microwave Theory and Techniques 58(1), 21–31 (2010)